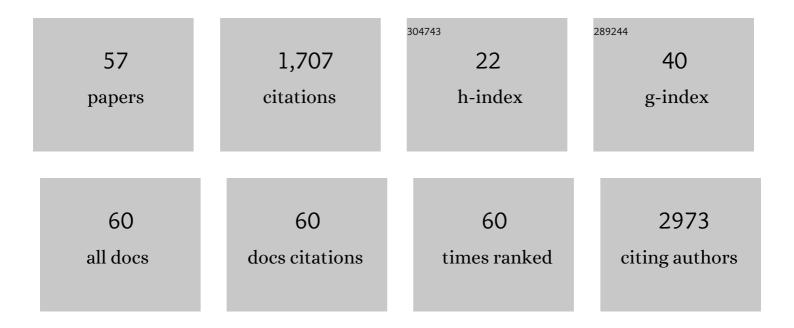
## **Emanuele Smecca**

List of Publications by Year in descending order

Source: https://exaly.com/author-pdf/6676787/publications.pdf Version: 2024-02-01



#	Article	IF	CITATIONS
1	Stability of solution-processed MAPbI <sub>3</sub> and FAPbI <sub>3</sub> layers. Physical Chemistry Chemical Physics, 2016, 18, 13413-13422.	2.8	208
2	Temperature-Dependent Optical Band Gap in CsPbBr <sub>3</sub> , MAPbBr <sub>3</sub> , and FAPbBr <sub>3</sub> Single Crystals. Journal of Physical Chemistry Letters, 2020, 11, 2490-2496.	4.6	173
3	Atomistic origins of CH3NH3PbI3 degradation to PbI2 in vacuum. Applied Physics Letters, 2015, 106, .	3.3	158
4	Pb clustering and PbI2 nanofragmentation during methylammonium lead iodide perovskite degradation. Nature Communications, 2019, 10, 2196.	12.8	116
5	Stability and Degradation in Hybrid Perovskites: Is the Glass Half-Empty or Half-Full?. Journal of Physical Chemistry Letters, 2018, 9, 3000-3007.	4.6	102
6	Similar Structural Dynamics for the Degradation of CH <sub>3</sub> NH <sub>3</sub> PbI <sub>3</sub> in Air and in Vacuum. ChemPhysChem, 2015, 16, 3064-3071.	2.1	80
7	First Evidence of CH <sub>3</sub> NH <sub>3</sub> Pbl <sub>3</sub> Optical Constants Improvement in a N <sub>2</sub> Environment in the Range 40–80 °C. Journal of Physical Chemistry C, 2017, 121, 7703-7710.	3.1	49
8	Nitrogen Soaking Promotes Lattice Recovery inÂPolycrystalline Hybrid Perovskites. Advanced Energy Materials, 2019, 9, 1803450.	19.5	46
9	Spectroscopic and Theoretical Study of the Grafting Modes of Phosphonic Acids on ZnO Nanorods. Journal of Physical Chemistry C, 2013, 117, 5364-5372.	3.1	45
10	Improvement of the fatigue resistance of NiTi endodontic files by surface and bulk modifications. International Endodontic Journal, 2010, 43, 866-873.	5.0	37
11	Spontaneous bidirectional ordering of CH3NH3+ in lead iodide perovskites at room temperature: The origins of the tetragonal phase. Scientific Reports, 2016, 6, 24443.	3.3	37
12	Revealing a Discontinuity in the Degradation Behavior of CH <sub>3</sub> NH <sub>3</sub> PbI <sub>3</sub> during Thermal Operation. Journal of Physical Chemistry C, 2017, 121, 13577-13585.	3.1	37
13	Texture of MAPbI <sub>3</sub> Layers Assisted by Chloride on Flat TiO <sub>2</sub> Substrates. Journal of Physical Chemistry C, 2015, 119, 19808-19816.	3.1	36
14	Multi-Scale-Porosity TiO2 scaffolds grown by innovative sputtering methods for high throughput hybrid photovoltaics. Scientific Reports, 2016, 6, 39509.	3.3	34
15	AIN texturing and piezoelectricity on flexible substrates for sensor applications. Applied Physics Letters, 2015, 106 Structural and electronic transitions in <mml:math< td=""><td>3.3</td><td>33</td></mml:math<>	3.3	33
16	xmlns:mml="http://www.w3.org/1998/Math/MathML"> <mml:mrow><mml:mi mathvariant="normal"&gt;G<mml:msub><mml:mi mathvariant="normal"&gt;e<mml:mn>2</mml:mn></mml:mi </mml:msub><mml:mi mathvariant="normal"&gt;S<mml:msub><mml:mi< td=""><td>3.2</td><td>33</td></mml:mi<></mml:msub></mml:mi </mml:mi </mml:mrow>	3.2	33
17	mathvariant="normal">b <mml:mn>2</mml:mn> <mml:mi mathvariant="normal"&gt; Local Order and Rotational Dynamics in Mixed A-Cation Lead Iodide Perovskites. Journal of Physical Chemistry Letters, 2020, 11, 1068-1074.</mml:mi 	4.6	31
18	Nanostructured TiO <sub>2</sub> Grown by Low-Temperature Reactive Sputtering for Planar Perovskite Solar Cells. ACS Applied Energy Materials, 2019, 2, 6218-6229.	5.1	27

#	Article	IF	CITATIONS
19	From PbI <sub>2</sub> to MAPbI <sub>3</sub> through Layered Intermediates. Journal of Physical Chemistry C, 2016, 120, 19768-19777.	3.1	26
20	CsPbBr <sub>3</sub> , MAPbBr <sub>3</sub> , and FAPbBr <sub>3</sub> Bromide Perovskite Single Crystals: Interband Critical Points under Dry N <sub>2</sub> and Optical Degradation under Humid Air. Journal of Physical Chemistry C, 2021, 125, 4938-4945.	3.1	26
21	Morphological and electrical properties of Nickel based Ohmic contacts formed by laser annealing process on n-type 4H-SiC. Materials Science in Semiconductor Processing, 2019, 97, 62-66.	4.0	25
22	Two-step MAPbl <sub>3</sub> deposition by low-vacuum proximity-space-effusion for high-efficiency inverted semitransparent perovskite solar cells. Journal of Materials Chemistry A, 2021, 9, 16456-16469.	10.3	25
23	Innovative spongy TiO2 layers for gas detection at low working temperature. Sensors and Actuators B: Chemical, 2018, 259, 658-667.	7.8	23
24	Low-cost high-haze films based on ZnO nanorods for light scattering in thin c-Si solar cells. Applied Physics Letters, 2015, 106, .	3.3	21
25	Performance of natural-dye-sensitized solar cells by ZnO nanorod and nanowall enhanced photoelectrodes. Beilstein Journal of Nanotechnology, 2017, 8, 287-295.	2.8	21
26	Engineered Si(100) surfaces for the gas-phase anchoring of metal β-diketonate complexes. Inorganica Chimica Acta, 2007, 360, 170-178.	2.4	19
27	Low temperature sputtered TiO <sub>2</sub> nano sheaths on electrospun PES fibers as high porosity photoactive material. RSC Advances, 2015, 5, 73444-73450.	3.6	14
28	Piezoelectric domains in BiFeO3 films grown via MOCVD: Structure/property relationship. Surface and Coatings Technology, 2013, 230, 168-173.	4.8	12
29	A Comparison Among Low Temperature Piezoelectric Flexible Sensors Based on Polysilicon TFTs for Advanced Tactile Sensing on Plastic. Journal of Display Technology, 2016, 12, 209-213.	1.2	12
30	Pervasive infiltration and multi-branch chemisorption of N-719 molecules into newly designed spongy TiO <sub>2</sub> layers deposited by gig-lox sputtering processes. Journal of Materials Chemistry A, 2017, 5, 25529-25538.	10.3	12
31	Ni/4H-SiC interaction and silicide formation under excimer laser annealing for ohmic contact. Materialia, 2020, 9, 100528.	2.7	12
32	Exploring the Structural Competition between the Black and the Yellow Phase of CsPbI3. Nanomaterials, 2021, 11, 1282.	4.1	12
33	Metalâ€Organic Chemical Vapor Deposition (MOCVD) Synthesis of Heteroepitaxial Pr <sub>0.7</sub> Ca <sub>0.3</sub> MnO <sub>3</sub> Films: Effects of Processing Conditions on Structural/Morphological and Functional Properties. ChemistryOpen, 2015, 4, 523-532.	1.9	10
34	Properties of Al2O3 thin films deposited on 4H-SiC by reactive ion sputtering. Materials Science in Semiconductor Processing, 2019, 93, 290-294.	4.0	10
35	Controlled Al3+ Incorporation in the ZnO Lattice at 188 °C by Soft Reactive Co-Sputtering for Transparent Conductive Oxides. Energies, 2016, 9, 433.	3.1	9
36	Outâ€ofâ€Glovebox Integration of Recyclable Europiumâ€Doped CsPbI <sub>3</sub> in Tripleâ€Mesoscopic Carbonâ€Based Solar Cells Exceeding 9% Efficiency. Solar Rrl, 2022, 6, .	5.8	9

**EMANUELE SMECCA** 

#	Article	IF	CITATIONS
37	Influence of hydrofluoric acid treatment on electroless deposition of Au clusters. Beilstein Journal of Nanotechnology, 2017, 8, 183-189.	2.8	8
38	New Synthetic Route for the Growth of α-FeOOH/NH <sub>2</sub> -Mil-101 Films on Copper Foil for High Surface Area Electrodes. ACS Omega, 2019, 4, 18495-18501.	3.5	8
39	Nitrogen doped spongy TiO2 layers for sensors application. Materials Science in Semiconductor Processing, 2019, 98, 44-48.	4.0	8
40	Full Efficiency Recovery in Hole-Transporting Layer-Free Perovskite Solar Cells With Free-Standing Dry-Carbon Top-Contacts. Frontiers in Chemistry, 2020, 8, 200.	3.6	8
41	Formation of CsPbI <sub>3</sub> γâ€Phase at 80 °C by Europiumâ€Assisted Snowplow Effect. Advanced Energy and Sustainability Research, 2021, 2, 2100091.	5.8	8
42	Blackâ€Yellow Bandgap Tradeâ€Off During Thermal Stability Tests in Lowâ€Temperature Euâ€Doped CsPbl <sub>3</sub> . Solar Rrl, 2022, 6, .	5.8	8
43	Spatially Confined Functionalization of Transparent NiO Thin Films with a Luminescent (1,10â€Phenanthroline)tris(2â€thenoyltrifluoroacetonato)europium Monolayer. European Journal of Inorganic Chemistry, 2015, 2015, 1261-1268.	2.0	7
44	Metal/P-GaN Contacts on AlGaN/GaN Heterostructures for Normally-Off HEMTs. Materials Science Forum, 0, 858, 1170-1173.	0.3	7
45	Bimodal Porosity and Stability of a TiO2 Gig-Lox Sponge Infiltrated with Methyl-Ammonium Lead Iodide Perovskite. Nanomaterials, 2019, 9, 1300.	4.1	7
46	Heterogeneous growth of continuous ZIF-8 films on low-temperature amorphous silicon. Applied Surface Science, 2019, 473, 182-189.	6.1	7
47	Improved Electrical and Structural Stability in HTL-Free Perovskite Solar Cells by Vacuum Curing Treatment. Energies, 2020, 13, 3953.	3.1	7
48	Tetra-anionic porphyrin loading onto ZnO nanoneedles: A hybrid covalent/non covalent approach. Materials Chemistry and Physics, 2014, 143, 977-982.	4.0	6
49	Simulation of the Growth Kinetics in Group IV Compound Semiconductors. Physica Status Solidi (A) Applications and Materials Science, 2019, 216, 1800597.	1.8	6
50	Optical behaviour of γ-black CsPbI <sub>3</sub> phases formed by quenching from 80 °C and 325 °C. JPhys Materials, 2021, 4, 034011.	4.2	6
51	A strategy to stabilise the local structure of Ti4+ and Zn2+ species against aging in TiO2/aluminium-doped ZnO bi-layers for applications in hybrid solar cells. Journal of Applied Physics, 2014, 116, .	2.5	5
52	High Resolution Investigation of Stacking Fault Density by HRXRD and STEM. Materials Science Forum, 0, 963, 346-349.	0.3	5
53	Porous Gig-Lox TiO2 Doped with N2 at Room Temperature for P-Type Response to Ethanol. Chemosensors, 2019, 7, 12.	3.6	4
54	Low-temperature flexible piezoelectric AlN capacitor integrated on ultra-flexible poly-Si TFT for		2

advanced tactile sensing. , 2014, , .

Emanuele Smecca

#	Article	IF	CITATIONS
55	Phase Transitions in Ge-Sb-Te Alloys Induced by Ion Irradiations. MRS Advances, 2016, 1, 2701-2709.	0.9	2
56	Structural and Electrical Characterization of Ni-Based Ohmic Contacts on 4H-SiC Formed by Solid-State Laser Annealing. Materials Science Forum, 0, 1062, 417-421.	0.3	2
57	MAPbI3 Deposition by LV-PSE on TiO2 for Photovoltaic Application. Frontiers in Electronics, 2021, 2, .	3.2	1